

CAN DUST EMISSION BE USED TO MAP THE INTERSTELLAR MEDIUM IN HIGH-REDSHIFT GALAXIES? RESULTS FROM THE HERSCHEL REFERENCE SURVEY

STEPHEN EALES¹, MATTHEW W. L. SMITH¹, ROBBIE AULD¹, MAARTEN BAES², GEORGE J. BENDO³, SIMONE BIANCHI⁴,
ALESSANDRO BOSELLI⁵, LAURE CIESLA⁵, DAVID CLEMENTS⁶, ASANTHA COORAY⁷, LUCA CORTESE⁸, JON DAVIES¹, ILSE DE
LOOZE², MAUD GALAMETZ⁹, WALTER GEAR¹, GIANFRANCO GENTILE², HALEY GOMEZ¹, JACOPO FRITZ², TOM HUGHES¹⁰,
SUZANNE MADDEN¹¹, LAURA MAGRINI⁴, MICHAEL POHLEN¹, LUIGI SPINOGLIO¹², JORIS VERSTAPPEN², CATHERINE
VLAHAKIS¹³, CHRISTINE D. WILSON¹⁴

submitted to ApJ

ABSTRACT

It has often been suggested that an alternative to the standard CO/21-cm method for estimating the mass of the interstellar medium (ISM) in a galaxy might be to estimate the mass of the ISM from the continuum dust emission. In this paper, we investigate the potential of this technique using Herschel observations of ten galaxies in the Herschel Reference Survey and in the Herschel Virgo Cluster Survey. We show that the emission detected by Herschel is mostly from dust that has a temperature and emissivity index similar to that of dust in the local ISM in our galaxy, with the temperature generally increasing towards the centre of each galaxy. We calibrate the dust method using the CO and 21-cm observations to provide an independent estimate of the mass of hydrogen in each galaxy, solving the problem of the uncertain ‘X factor’ for the molecular gas by minimizing the dispersion in the ratio of the masses estimated using the two methods. With the calibration for the dust method and the estimate of the X-factor produced in this way, the dispersion in the ratio of the two gas masses is 30%, which gives an upper limit on the fundamental accuracy of the dust method. The calibration we obtain for the dust method is very similar to an independent Herschel measurement for M31 and to the calibration for the Milky Way from Planck measurements.

Subject headings: galaxies: ISM — submillimetre

1. INTRODUCTION

In order to understand the physics and evolution of galaxies, accurate measurements of their gas content are absolutely crucial: stars produce most of the energy output of galaxies and they form out of this reservoir of gas. Unfortunately there are problems with all the tech-

niques for observing the different phases of the interstellar medium (ISM). Probably the most reliable technique is to use the 21-cm line to map the atomic phase, but if the gas becomes optically thick the linear relationship between the line brightness and the column density of gas breaks down (Braun et al. 2009). The mass of the molecular phase is usually estimated from the 1-0 line of the tracer CO molecule, but the constant of proportionality between the two - the ‘X-factor’ - is notoriously uncertain (Bell et al. 2007), and there is evidence that it depends on metallicity (Wilson 1995; Israel 2005; Boselli et al. 2002) and possibly on other factors (Israel 1997). An additional problem with the standard CO/21-cm method is that recent observations with Fermi and Planck imply that a significant fraction of the gas in the Galaxy consists of ‘dark gas’ traced by neither line (Abdo et al. 2010; Planck Collaboration 2011a). There is also the practical problem that with current telescopes it is difficult to detect either line from galaxies at $z > 0.1$.

As early as the mid-eighties (Hilderbrand 1983) it was suggested that one way to estimate the mass of the ISM in a galaxy might be from the optical depth of the submillimetre continuum emission from the dust; dust grains are robust and found in all phases of the ISM and the continuum dust emission is generally optically thin. More recent attempts to use the dust emission to infer the gas distribution are described in Boselli et al. (2002) and in Guélin et al. (1993, 1995). The reason why this method is of topical interest is that the Herschel Space Observatory (Pilbratt et al. 2010) is in the process of measuring the continuum dust emission from hundreds of thousands of galaxies, seen over 10 billion years of cosmic history (Eales et al. 2010a; Oliver et al. 2011), and it

¹ School of Physics and Astronomy, Cardiff University, Queens Buildings, The Parade, Cardiff CF24 3AA, UK

² Sterrenkundig Observatorium, Universiteit Gent, Krijgslaan 281 S9, B-9000 Gent, Belgium

³ UK ALMA Regional Centre Node, Jodrell Bank Centre for Astrophysics, School of Physics and Astronomy, University of Manchester, Oxford Road, Manchester M13 9PL, UK

⁴ INAF-Osservatorio Astrofisico di Arcetri, Largo E. Fermi 5, 50125, Firenze, Italy

⁵ Laboratoire d’Astrophysique de Marseille, UMR6110 CNRS, 38 rue F. Joliot-Curie, F-1338 Marseille, France

⁶ Astrophysics Group, Imperial College, Blackett Lab, Prince Consort Road, London SW7 2AZ, UK

⁷ Dept. of Physics & Astronomy, Univ. of California, Irvine, CA 92697, USA

⁸ European Southern Observatory, Karl-Schwarzschild-Strasse 2 D-85748, Garching bei München, Germany

⁹ Institute of Astronomy, University of Cambridge, Madingley Road, Cambridge CB3 0HA, United Kingdom

¹⁰ Kavli Institute for Astronomy & Astrophysics, Peking University, Beijing 100871, China

¹¹ Laboratoire AIM, CEA/DSM - CNRS - Université Paris Diderot, Irfu/Service d’Astrophysique, 91191 Gif sur Yvette, France

¹² Istituto di Fisica dello Spazio Interplanetario, Istituto Nazionale di Astrofisica, Via Fosso del Cavaliere 100, I-00133 Roma, Italy

¹³ Joint ALMA Office, Alonso de Cordova 3107, Vitacura, and Departamento de Astronomía, Universidad de Chile, Casilla 36-D, Santiago, Chile

¹⁴ Department of Physics & Astronomy, McMaster University, Hamilton, Ontario L8S 4M1, Canada

will never be practical to estimate the mass of the ISM in so many galaxies using the standard 21-cm/CO method. Although ALMA will improve this for CO observations, it will still not be feasible to measure the strength of the CO line in thousands of high-redshift galaxies. A recent Herschel result has given additional encouragement that this method may be a useful one, since Corbelli et al. (2011) have shown that in a sample of galaxies in the Virgo cluster dust mass is more tightly correlated to the total gas mass than to the masses of molecular or atomic gas separately.

To apply the dust method, of course, it is necessary to know the temperature of the dust, but this is a practical problem with the method rather than a fundamental one, and in principle it can be solved with accurate measurements of the continuum emission at enough far-infrared wavelengths to cover the peak of the emission. An additional practical problem is that there is evidence that the ratio of dust emission to gas mass depends on the metallicity of the gas (Lisefeld & Ferrara 1998; James et al. 2002; Draine et al. 2007), although this is obviously also a problem with the alternative method, which uses the CO line to trace the molecular phase.

One way to try to calibrate the relationship between the submillimetre optical-depth and the mass of the ISM is to do it in two steps: first obtain a relationship between the optical depth and the mass of dust; then obtain a relationship between the mass of dust and the mass of the ISM. The problem with this approach is that the uncertain radiative efficiency of dust grains (Draine 2003) and the lack of a reliable independent method of measuring the gas-to-dust ratio in galaxies mean that there are difficulties in both steps (Hildebrand 1983). In this paper we adopt the more direct approach of ignoring the properties of the dust grains and calibrating the relationship between gas mass and dust optical depth directly. Recent Planck results suggest this is a promising method. The Planck team finds the relationship between submillimetre optical depth and gas column density is independent of Galactic radius and the same in both the atomic and molecular phases (Planck Collaboration 2011b,c).

In this paper, we use Herschel observations with SPIRE (Griffin et al. 2010) and PACS (Poglitsch et al. 2010) of ten nearby galaxies taken from the Herschel Reference Survey (Boselli et al. 2010) and the Herschel Virgo Cluster Survey (Davies et al. 2010) to estimate the relationship between the dust optical-depth and the mass of gas in each galaxy.

2. THE METHOD

The Planck team (Planck Collaboration 2011b) has recently used Planck observations of the continuum emission from the dust to examine the relationship between the optical depth of continuum emission from dust and the column density of gas as a function of Galactic radius. Using an X-factor for the molecular phase of $1.8 \times 10^{20} \text{cm}^{-2} (\text{Kkm s}^{-1})^{-1}$, which is consistent with recent studies of the diffuse gamma-ray emission in the Galactic plane (Abdo et al. 2010; Ackermann et al. 2011), the Planck team found the following relationship at the solar circle:

$$\tau = 1.1 \times 10^{-25} \left(\frac{\lambda}{250 \mu\text{m}} \right)^{-1.8} N_H \quad (1)$$

in which τ is the optical depth at wavelength λ and N_H is the column density of hydrogen measured in atoms cm^{-2} . The team found that this relationship is independent of Galactic radius and is the same in the molecular and atomic phases, although this latter conclusion depends on the value of the X-factor being correct. The relationship above is very similar to the result from the Planck and COBE observations of dust at high Galactic latitude (Planck collaboration 2011c; Boulanger et al. 1996). The Planck team found a value of the dust-emissivity index, β , of 1.8, which is independent of Galactic radius, and they showed that the temperature of dust in the atomic phase falls with Galactic radius, with a value of 17.6 K at the solar circle (Planck Collaboration 2011b). The relationship above can be translated (Appendix 1) into the following relationship between mass of hydrogen, M_H , and monochromatic submillimetre luminosity (L_ν):

$$M_H = \eta_c \times \frac{1.52 \times 10^2 \times L_\nu}{B_\nu(T_d) \times \left(\frac{\lambda}{250} \right)^{-1.8}} \quad (2)$$

We have put everything in equation (2) in S.I. units except wavelength (λ), which is measured in microns. Luminosity is measured in Watts $\text{Hz}^{-1} \text{sr}^{-1}$. We have introduced a constant, η_c , into the equation. This is equal to one for the Milky Way. Our objective in this paper is to measure η_c for external galaxies.

3. THE CALIBRATION SAMPLE AND THE DATA

Our main aim in this initial paper is not to provide a practical method for estimating the gas masses of high-redshift galaxies, which would require a study of a very large sample of galaxies covering a wide range of metallicity and other parameters, but to investigate the ultimate potential of this method. The biggest practical difficulty in using this method is in measuring accurate dust temperatures. Although the effect of an error in the dust temperature on the estimate of the dust mass is much less at the longest Herschel wavelength, 500 μm , than at the wavelengths used by previous space observatories, it is still approximately linear, a 10% error in the dust temperature leading to a $\simeq 10\%$ error in the dust mass. There is an additional problem if there is a mixture of dust at different temperatures within the telescope beam; the dust temperature obtained by fitting a single-temperature modified blackbody to this dust will then be systematically too high, leading to a systematic underestimate of the dust mass (Eales, Wynn-Williams and Duncan 1989; Shetty et al. 2009a). To overcome this problem as much as possible, we have restricted this initial pilot study to galaxies that are well resolved by Herschel. There is a strong temperature gradient in the dust in the Milky Way (Planck Collaboration 2011b) and we will show in this paper that this is also true for most of the galaxies we have studied. Therefore global submillimetre observations of a galaxy will almost certainly contain dust with a range of temperatures, which will be a practical problem in using this method to estimate the mass of the gas in high-redshift galaxies detected by Herschel. However, by restricting our study to galaxies which are large enough that we can investigate the distribution of dust temperature within each galaxy, we have

TABLE 1
SAMPLE

Galaxy	D/Mpc	12 + log(O/H)	PACS	N	$\langle \beta \rangle$	$\langle T \rangle$	$r_s(\beta, r)$	$r_s(T, r)$
NGC4192 (M98)	16.8	8.76±0.08	Y	29	2.11±0.04	15.5±0.2	0.21	-0.56
NGC 4254 (M99)	16.8	8.71±0.13	Y	44	2.20±0.02	17.6±0.3	-0.10	-0.48
NGC 4321 (M100)	16.8	8.75±0.05	Y	53	2.56±0.04	15.5±0.2	0.39	-0.63
NGC 4402	16.8	8.67±0.02	Y	10	2.17±0.09	19.7±0.7	-0.23	0.20
NGC 4419	16.8	...	N	7	2.20±0.08	21.5±0.6	0.02	-0.10
NGC 4535	16.8	8.75±0.05	Y	35	2.24±0.02	16.1±0.3	0.43	-0.65
NGC 4536	16.8	8.71±0.08	N	42	1.43±0.04	24.9±0.1	-0.73	-0.22
NGC 4569 (M90)	16.8	...	N	19	2.29±0.05	19.5±0.3	0.39	-0.61
NGC 4579 (M58)	16.8	...	Y	26	2.26±0.06	17.4±0.3	0.31	-0.78
NGC 4689	16.8	8.66±0.05	N	16	2.11±0.06	20.1±0.3	-0.72	-0.07
M31	0.7	...	Y	3150	1.93	17.3

NOTE. — Reading from the left, the columns are: Col. 1—name; col. 2—distance in Mpc; col. 3—oxygen abundance estimated from optical drift-scan spectroscopy by Hughes et al. (2011). For each galaxy, one or more estimates of the oxygen abundance have been made using different line ratios and the calibrations described in Kewley & Ellison (2008), which use the O3N2 calibration from Pettini & Pagel (2004) as the base calibration. The abundances given in the table are the means of these estimates. Col. 4—whether the galaxy has PACS observations; col. 5—number of pixels with S/N at 500 μm greater than 10; col. 6—mean value of β for galaxy; col. 7—mean value of temperature for galaxy; col. 8—Value of Spearman rank coefficient for relationship between β and galactocentric radius; col. 9—Value of Spearman rank coefficient for relationship between temperature and galactocentric radius.

attempted to minimise this effect, in order to explore the ultimate limits of this technique.

The sample is mostly drawn from two Herschel key projects: the Herschel Reference Survey (HRS), a survey with SPIRE at 250, 350 and 500 μm of 323 galaxies in a magnitude-limited and volume-limited sample of the local Universe (Boselli et al. 2010a), and the Herschel Virgo Infrared Cluster Survey (HeVICS, Davies et al. 2010), a survey of the Virgo Cluster at 110 and 160 μm with PACS and at 250, 350 and 500 μm with SPIRE. Our method requires high-quality maps made in the CO 1-0 line and in the 21-cm line, which cuts us down to 10 galaxies that have both been mapped in CO 1-0 at the Nobeyama Radio Observatory (Kuno et al. 2007) and in the 21-cm line by the VLA as part of the VIVA survey (VLA Imaging of Virgo in Atomic Gas - Chung et al. 2009). A requirement for our method is that we need observations at $\lambda < 250 \mu\text{m}$ to determine the dust temperature. Six of the galaxies are common to HRS and HeVICS and so have PACS observations; for the others we have used archival Spitzer observations at 70 μm , reprocessed as described by Bendo et al. (2011). The reduction of the SPIRE and PACS data for the two key projects is described by Smith et al. (2011a) and Davies et al. (2011).

Table 1 lists the galaxies and their basic properties. Figure 1 shows a montage of the 250- μm images of the galaxies. Although this sample is not representative of the entire galaxy population, consisting of galaxies in the Virgo Cluster, we have partly mitigated this problem by also considering two other galaxies: our own (through the Planck observations) and the other big spiral in the Local Group, M31. The analysis of the gas and dust in M31 is presented elsewhere (Smith et al. 2011b) and we simply give the necessary results here.

4. THE TEMPERATURE OF THE DUST IN THE GALAXIES

We smoothed all the images to the resolution of the lowest-resolution image, the 500 μm image, using the method described in Bendo et al. (2010). We then re-gridded all the images on to a pixel scale of 36 arcsec,

which is the size of the 500- μm beam (FWHM), ensuring that the data in each pixel is largely, although not completely, independent. We estimated the dust temperature by fitting single-temperature modified blackbodies ($F_\nu \propto B_\nu(T_d)\nu^\beta$) to the measured fluxes for each pixel, allowing the dust temperature (T_d) and the dust emissivity index (β) to vary independently and minimizing the χ^2 statistic. We restricted all our analysis to pixels in which the emission in each band was detected at $> 5\sigma$. Where PACS data existed, we fitted the modified blackbodies to the 100-500 μm flux densities, and for the other galaxies we used the Spitzer 70- μm image and the 250, 350 and 500 μm measurements. We fitted the modified blackbody to the measured flux densities after convolving it with the appropriate filters and after applying, for the SPIRE wavelengths, the ‘K4’ correction (SPIRE Observers’ Manual). For the SPIRE measurements, we used the filter functions given for extended sources in the SPIRE Observers’ Manual. In calculating the χ^2 statistic, we assumed 20% calibration uncertainties for PACS and Spitzer and two calibration errors for the SPIRE measurements, one of 5% correlated over the three bands and one of 5% uncorrelated between the bands (SPIRE Observers’ Manual). We estimated the flux errors in each pixel by adding in quadrature the calibration error and the r.m.s. dispersion in the pixel values in an annulus around the galaxy.

For nine of the galaxies we found that the χ^2 values of the fits showed that a single-temperature modified blackbody is an adequate representation of the data. For M100 we found 20% of the pixels had $\chi^2 > 2.71$, whereas we would have expected 10% by chance, so that for this galaxy there is evidence that the dust emission from some pixels may not be adequately represented by a single-temperature modified blackbody. Submillimetre observations of some dwarf galaxies have found excess emission at long wavelengths, which may indicate a large amount of very cold dust, a change in the dust emissivity at long wavelengths, or for which there may be some other explanation (Galametz et al. 2011). This excess has not been seen in the HRS galaxies (Boselli et al. 2010b). Nevertheless, we looked for evidence for

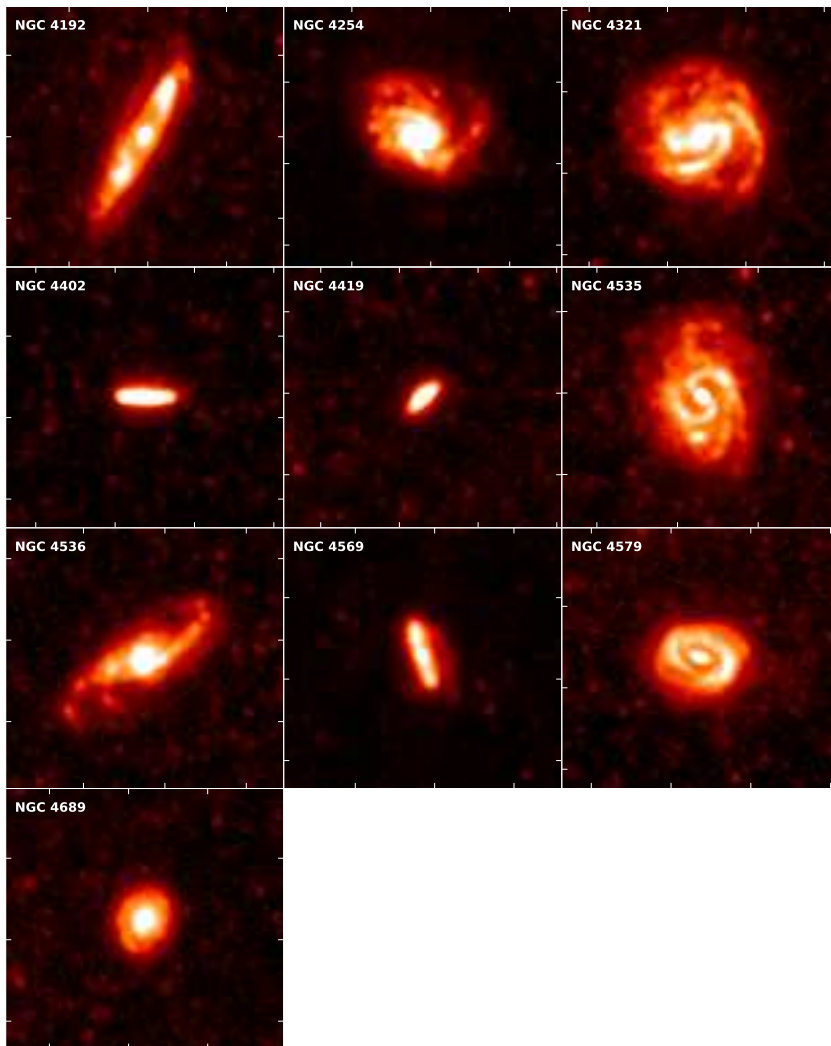


FIG. 1.— Images at $250\mu\text{m}$ of the galaxies in the calibration sample. The tick marks are at an interval of 3 arcmin.

this in our sample by measuring $(F_{500\mu\text{m}} - F_{\text{model}})/\sigma$ for each pixel, in which $F_{500\mu\text{m}}$ is the flux density at $500\mu\text{m}$, F_{model} is the flux at that wavelength given by the best-fitting model, and σ is the noise. In calculating σ we have not included the part of the calibration error that is correlated between bands. Fig. 2 shows a histogram of this quantity for all the pixels. There is no evidence in these galaxies for any excess emission at $500\mu\text{m}$.

We estimated errors on each estimate of temperature and β using the method of Avni (1976). Table 1 gives the weighted averages of the temperature and β for each galaxy. We have also included estimates of these quantities for M31 (Smith et al. 2011b), using the same technique as here. With the exception of NGC 4536, the values of $\langle T_d \rangle$ are similar to the values for the local interstellar dust estimated by COBE (17.5K - Boulanger et al. 1996) and by Planck (17.9K - Planck Collaboration 2011c) and to the average value for the dust in M31 (17.3 K - Smith et al. 2011b). The similarity of the values of T_d and the results of other recent Herschel

studies (Bendo et al. 2011a, Foyle et al. 2011; Smith et al. 2011b) suggest that a very large fraction of the dust emission at $\lambda > 100\mu\text{m}$ is from dust grains heated by the general interstellar radiation field rather than from dust grains in the warmer environment of a star-formation region. We do not address here the question of whether this general interstellar radiation field is dominated by the light from old stars (Bendo et al. 2011a) or whether it is dominated by the light from the young OB stars (Foyle et al. 2011). The values of $\langle \beta \rangle$ are slightly but systematically higher than the values for the Milky Way (1.8 - Planck Collaboration 2011b,c) and for M31 (1.93 - Smith et al. 2011). We could possibly explain the difference with the Planck results by some calibration issue between Planck and Herschel, but the results for M31 have been obtained using similar data and method to that used here. We do not have an explanation for the difference, but it is possibly relevant that most of the gas in the Virgo galaxies is in the molecular phase whereas most of the gas in M31 is in the atomic phase although

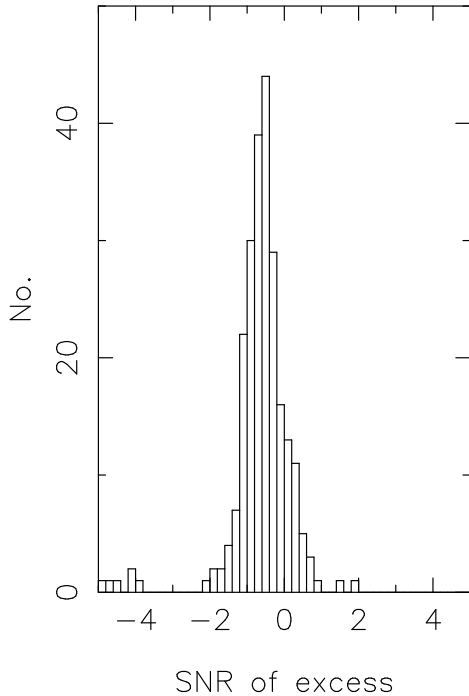


FIG. 2.— Histogram for all pixels for which we fitted a modified blackbody of $(F_{500\mu\text{m}} - F_{\text{model}})/\sigma$ in which $F_{500\mu\text{m}}$ is the measured flux at $500\ \mu\text{m}$, F_{model} is the flux predicted by the single-temperature modified blackbody, and σ is the error (including the part of the calibration error that is not correlated between bands but not the part that is correlated between bands). There is no evidence for any excess emission at $500\ \mu\text{m}$.

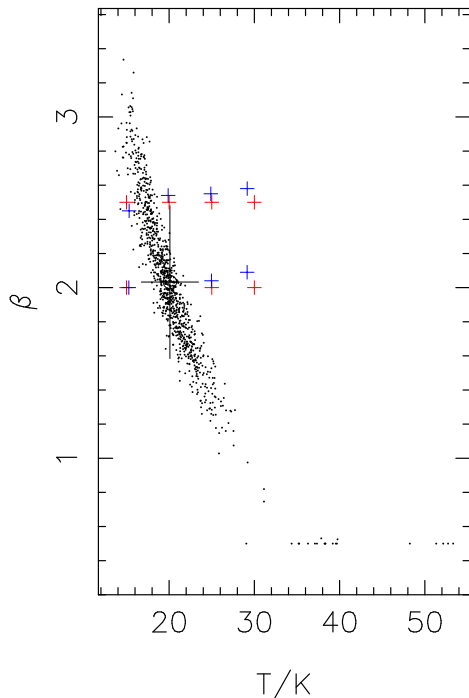


FIG. 3.— The results of a Monte-Carlo simulation in which we start with a single-temperature modified blackbody with a $500\text{-}\mu\text{m}$ flux typical of the pixels in the disk of M100, add typical noise, and then use our fitting procedure to estimate the values of T_d and β . The black points show the results for $T_d = 20\text{K}$ and $\beta = 2$ with the large cross showing the variance of the distribution along both axes. The red crosses show the other combinations of T_d and β we tried, and the blue crosses show the mean values of the estimates from the fits.

it is not obvious why this should produce a change in β .

We made a rough estimate of possible systematic errors in the dust temperature by repeating the analysis for the six galaxies with PACS observations but omitting the measurements in the $100\ \mu\text{m}$ band. One effect of fitting the model to only four flux measurements ($160\text{-}500\ \mu\text{m}$) is to increase the statistical errors on the dust temperatures by a factor of $\simeq 2$. There is no clear direction to changes in the estimates of the dust temperature: for three galaxies the temperature estimate increases and for three it decreases. The temperature change has a mean of $\delta T = 0.70\text{K}$ and a standard deviation of 1.17K , leading to a change in the estimate of the mass of the ISM with a mean of 6% and a standard deviation of 12% .

We can investigate further that the dust emission is adequately represented by dust at a single temperature by taking advantage of a well-known problem with this kind of analysis. If there is a range of dust temperature along the line-of-sight for a particular galaxy, the values of temperature and β produced by fitting a modified blackbody will be systematically too high and too low, respectively, which for an individual galaxy will lead to an underestimate of the dust mass. The important clue that this is a significant problem within a sample of galaxies is an inverse relationship between β and temperature (Shetty et al. 2009a). Before we can look for this relationship, we need to model another well-known problem: that the fitting procedure itself can produce a spurious β - T relationship (Shetty et al. 2009b). Figure 3 shows the results of a 1000-run Monte-Carlo simulation in which we start with a single-temperature modified blackbody with a $500\text{-}\mu\text{m}$ flux typical of one of the pixels in the disk of M100, add noise typical of these pixels, and then use our fitting procedure to estimate β and T . As expected, the fitting procedure produces a strong inverse correlation between β and T . However, the average value for both β and T that is recovered from the simulation is always very close to the input values, showing that there is no systematic bias in the results of our fits.

Figure 4 shows the measured value of $\langle T \rangle$ and $\langle \beta \rangle$ plotted against each other for each galaxy. Although the errors on the average values for the two quantities are still correlated, the figure shows that the errors are much smaller than the range of values for the two quantities. Any inverse correlation between the average quantities might then indicate the line-of-sight problem: the existence of dust at a range of temperatures in the galaxies with the ratio of warm-to-cold dust varying between the galaxies. There is no strong relationship between the two, with one obvious outlier, the galaxy NGC 4536. For NGC 4536, we used a Spitzer $70\text{-}\mu\text{m}$ flux, and it seems likely that in this individual case the low value of β and the high temperature are signs that much of the $70\text{-}\mu\text{m}$ flux is from dust that is warmer than the bulk of the dust. Therefore, for this galaxy it seemed likely that the estimate of the gas mass from the dust emission would be too low, and so we decided to omit NGC 4536 from the calibration sample. The other anomalous galaxy is M100 at the top of the diagram, but since there was no a priori reason to believe that a high value of β will lead to an overestimate of the dust mass and consequently of the gas mass, we retained this galaxy in the sample.

Figure 5 shows T_d and β plotted against the distance from the centre of each galaxy, and Table 1 gives the

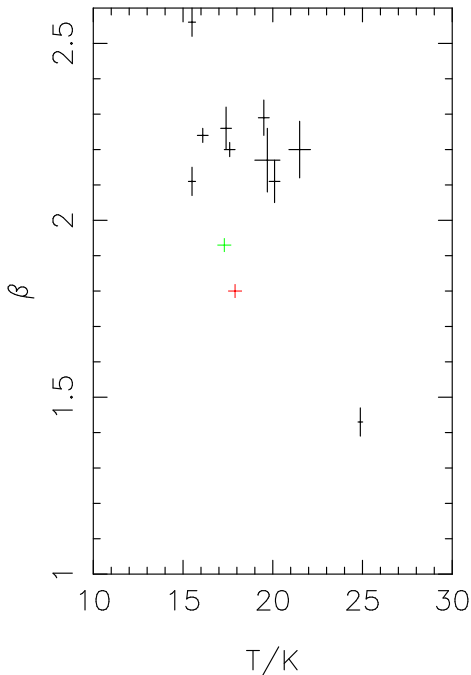


FIG. 4.— The mean values of T and β for the galaxies in Table 1. The crosses for these galaxies show the sizes of the 1σ errors on the means. The red cross shows the estimated values of T and β from the Planck observations of high-latitude dust in the Milky Way (Abergel et al. 2011) and the green cross shows the average values of T and β for M31, estimated using the same method we have employed here (Smith et al. 2011b).

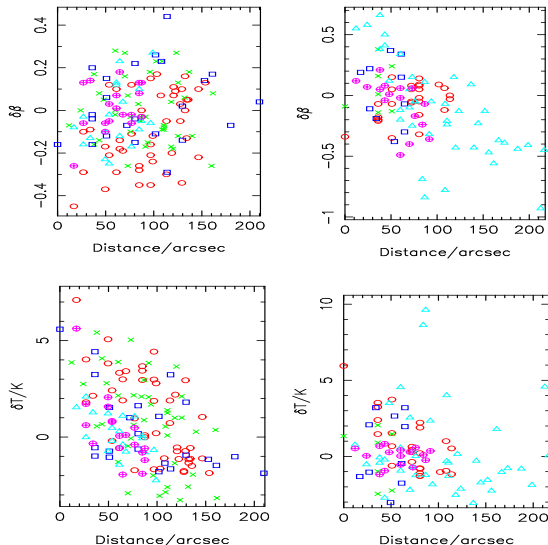


FIG. 5.— Plots of β (top) and temperature (bottom) versus radius for each galaxy. For each galaxy, the quantity plotted is the difference between the value of β or temperature in a pixel and the average value for that galaxy. The two panels on the left are for M100 (red circles), M99 (green crosses), M98 (blue squares), M90 (light blue triangles) and M58 (red crosses in circles). The two panels on the right are for NGC 4535 (red circles), NGC 4419 (green crosses), NGC 4402 (blue squares), NGC 4536 (light blue triangles) and NGC 4689 (red crosses in circles).

value of the Spearman correlation coefficient for each correlation. For eight of the remaining nine galaxies, there is a trend for T to increase towards the centre of each galaxy (significant in five cases), which can be qualitatively explained by the increase in the intensity of the interstellar radiation field towards the centre of a galaxy. This is similar to the radial gradient in dust temperature measured by the Planck team for the Milky Way (Planck Collaboration 2011b). The correlations between β and galactocentric distance are generally weaker and not in a consistent direction. Since the errors on the estimates of T and β for individual pixels are large, and because there is no compelling evidence for the variation of β within these galaxies, in the rest of the analysis we assume the value of β for each galaxy is a constant and use the value given in Table 1.

5. CALIBRATING THE METHOD

The mass of hydrogen can be estimated from equation (2). It can also be estimated in the standard way from the CO and HI lines:

$$M_{H, meth 2} = M(HI) + \left(\frac{X}{2 \times 10^{20}}\right)M(H_2) \quad (3)$$

in which $M(H_2)$ is the mass of molecular gas estimated using an X factor of $2 \times 10^{20} \text{ cm}^{-2}(\text{K km s}^{-1})^{-1}$ (Bolatto et al. 2008).

If we knew the value of the X-factor, we could estimate η_c for each galaxy by taking the ratio of the masses estimated from the two equations. The mean value would then give us the average calibration for the dust method, with the variance giving us an estimate of the usefulness of the method. Unfortunately, we don't, the uncertainty in the X-factor being a perennial irritation in extragalactic astronomy (Bell et al. 2007).

We have tried to overcome this problem by making the hypothesis that there is a universal value of X and η_c , at least for these nine galaxies, and finding the minimum chi-squared discrepancy from this hypothesis. When estimating the gas mass from equation (2), we used only pixels for which the $500\text{-}\mu\text{m}$ flux is detected at $> 10\sigma$ and estimated a temperature for each pixel by fitting a single-temperature modified blackbody to the fluxes for that pixel with the value of β from Table 1. We used the flux at $500 \mu\text{m}$ because the sensitivity of this method to errors in dust temperature decreases with wavelength. Our estimate of the gas mass for each galaxy is then the sum of the values for the individual pixels.

Before making the alternative estimate of the gas mass from the CO/HI method, we convolved the HI and CO maps to the same resolution as the Herschel images and put them on the same pixel scale. When estimating the gas mass from equation (3) we used the same pixels that were used for estimating the gas mass from the dust method. We estimated a total mass of atomic hydrogen for each galaxy by summing the values in the HI map in these pixels and a total mass of molecular hydrogen by summing the values in the CO map for these pixels.

To apply the chi-squared method it is necessary to make some assumption about the errors in the estimates of M_H in equation (2) and of $M(HI)$ and $M(H_2)$ in equation (3). We assumed errors of 10% in the estimates

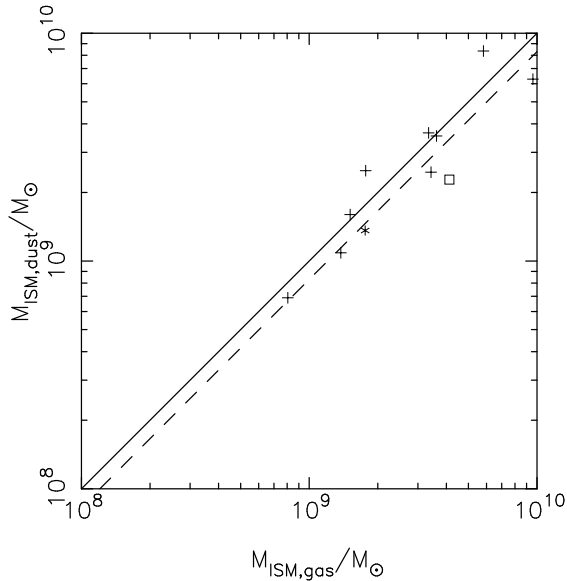


FIG. 6.— The gas masses derived using the two alternative methods using our best-fit values of the X factor and η_c . The crosses show the values for the nine galaxies in our calibration sample. The star shows the values for M31 and the square shows the value for NGC 4536. The solid line shows where the two gas masses are equal. The dashed line shows the relationship predicted using the calibration from the Planck observations of the Milky Way (Planck Collaboration 2011b).

of the total M_H for each galaxy obtained using the dust method, and we assumed the same error for the total mass obtained from the HI image. Based on our inspection of the CO maps, we concluded that the errors in $M(H_2)$ are likely to be larger, and we conservatively assumed that the errors in the total $M(H_2)$ for each galaxy are 30%. We estimated the error in our estimate of η_c using the method of Avni (1976), assuming there is one ‘useful’ parameter.

We varied X between 0.1 and 10, finding the best agreement with the model (minimum chi-squared) with $X=1.95$ and $\eta_c = 1.21$, with an upper 1σ limit of 1.41 and a lower 1σ limit of 1.07. If we omit the three galaxies without PACS measurements, we find best agreement with the model with $X=2.93$ and $\eta_c = 1.44$ with an upper limit 1σ limit of 1.71 and a lower 1σ limit of 1.28, slightly larger but consistent with the value for the full sample. Figure 6 shows the two estimates of the hydrogen mass plotted against each other for all the galaxies. We have included estimates for NGC 4536, although we did not use it to estimate η_c ; as expected, the mass of hydrogen estimated from the dust emission is systematically lower than for the other galaxies. We have also included in the figure estimates of the hydrogen mass for M31, using the same procedure and the same values of η_c and the X factor as for the other galaxies.

Using the estimate for the full sample, we can rewrite equation (2) in a simpler way:

$$M_H = k \frac{L_\nu}{B_\nu(T_d)} \quad (4)$$

in which our estimate of k is 640 kg m^{-2} at $500 \mu\text{m}$ with an uncertainty of approximately 20%. We have not used our method to estimate η_c at 250 and $350 \mu\text{m}$ because

of the larger effect of temperature errors at these wavelengths. However, we can make an approximate estimate of the values of k at these wavelengths by scaling by $\nu^{-\beta}$, using the median value of β in Table 1 (2.20). This gives values of k at 250 and $350 \mu\text{m}$ of 139 and 292 kg m^{-2} , respectively.

6. DISCUSSION

We can obtain an upper limit on the intrinsic error of our proposed method of using the continuum dust emission to estimate the gas mass by calculating the dispersion in Figure 6 of the ratio of the gas masses calculated using the two methods. The standard deviation of $\log_{10} \frac{M_{H,\text{meth } 1}}{M_{H,\text{meth } 2}}$ is 0.11, which gives an upper limit on the intrinsic error in estimating the mass of the gas from the dust emission of 30%. This is an upper limit, because this error term is also made up of observational errors and other possible astrophysical effects, such as variations in the X factor from galaxy to galaxy and differing amounts of CO-dark gas. However, even if we take this upper limit as an actual estimate of the error in this technique, the method is still clearly potentially useful for estimating the mass of the gas in the hundreds of thousands of high-redshift Herschel sources for which it will never be possible to make CO observations.

There are several limitations in our work. First, our sample does not represent very well the entire galaxy population, since all the galaxies are in the Virgo Cluster with metallicities close to the solar value (Table 1). The fact that both M31 and the Milky Way effectively have similar values of η_c (Fig. 6) is evidence that the cluster membership is not leading to significant bias, but the metallicity issue is an important one because one would expect η_c to have a dependence on metallicity (James et al. 2002; Draine et al. 2007; Corbelli et al. 2011). The relationship will be difficult to determine by simply comparing the gas masses derived using the two methods, because the X-factor is also likely to have a dependence on metallicity (Wilson 1995; Arimoto et al. 1996; Boselli et al. 2002; Israel 2005; Magrini et al. 2011. See Bolatto et al. [2008] for an alternative view), which also means of course that the metallicity issue does not give the standard CO/HI method a clear advantage for estimating the masses of the gas in high-redshift galaxies. Nevertheless, despite the difficulty, for turning this method into a practical one for estimating the masses of the gas in high-redshift galaxies, it will be important to carry out a similar analysis to the one in this paper but for a much larger sample of galaxies, with a wider range of properties, especially metallicity.

This is work for the future, but we note that a major difficulty is that there are very few absolute measurements of the metallicity in external galaxies. Most studies have relied on relationships between line ratios and metallicity that have been calibrated from absolute measurements or theoretical models, and uncertainties in these calibrations lead to an uncertainty in the metallicity of a factor of $\simeq 4$ (Moustakas et al. 2010; Hughes et al. 2011; Magrini et al. 2011). We note in passing that the uncertainty in metallicity is a major problem with estimating the mass-opacity coefficient of the dust using the method of James et al. (2002) and Eales et al. (2010b), since this method relies on accurate mea-

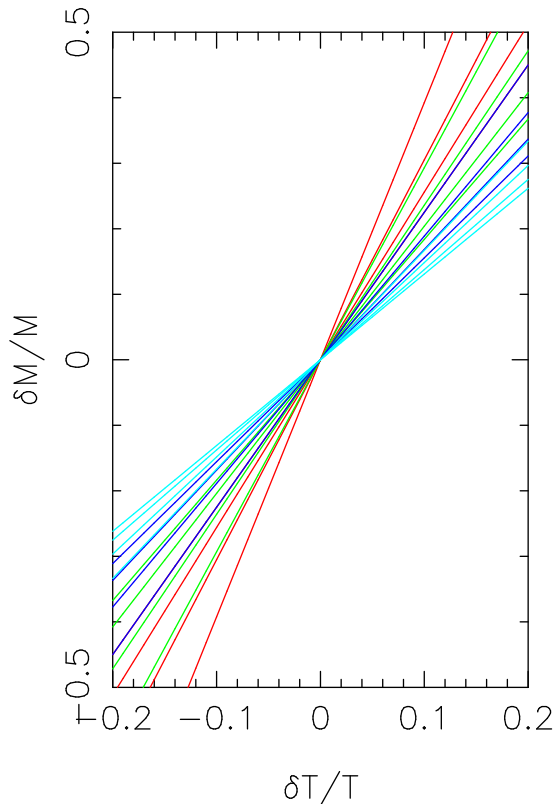


FIG. 7.— Plot showing the effect of an error in the estimate of dust temperature on the estimate of the mass of dust in a galaxy. The different colours correspond to different wavelengths: red—250 μm ; green—350 μm ; dark blue—500 μm ; light blue—850 μm . Curves are plotted for four dust temperatures: 15K, 20K, 25K and 30K. For any particular wavelength and fractional temperature error, the effect on the estimate of the dust mass is greatest for the coldest temperature.

measurements of the metallicity in external galaxies relative to the local ISM in our galaxy. Eales et al. (2010b) estimated a mass-opacity coefficient from Herschel observations of M99 and M100, finding a value much lower than predicted by dust models. Hughes et al. (2011) have recently made new estimates of the metallicity of the gas in M99 and M100 from existing data and find values four times greater than the values used in Eales et al. (2010b), accounting for this discrepancy.

A second problem is that we have calibrated the dust method using the standard CO/21-cm method, but if the latter method is missing CO-dark gas, there will be a bias in our calibration. This is not such a simple problem to overcome because it requires observations of this gas phase in nearby galaxies, which is difficult but can probably be done with observations in the [CII] 158.9- μm line with Herschel and SOFIA.

We also emphasise that for this method to be effective it is important to have accurate and unbiased estimates of the temperature of the dust. Fig. 7 shows how the percentage error in gas mass depends on the percentage error in the dust temperature for different rest-frame wavelengths and dust temperatures. The effect of an error in dust temperature increases with decreasing wavelength, and so in applying this method it is crucial to measure the monochromatic luminosity at the longest possible wavelength. For galaxies at $z > 1$, the effect of

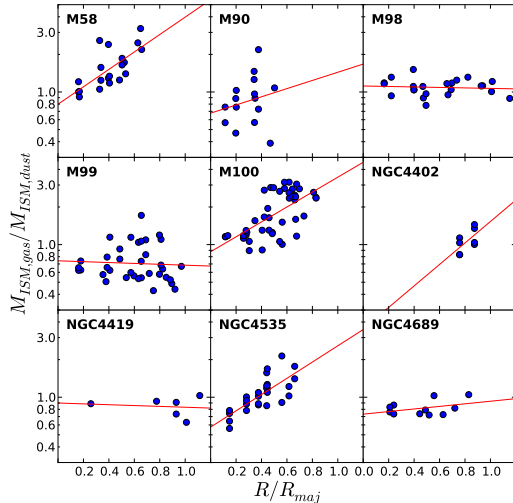


FIG. 8.— Plots of the ratio of the two estimates of the gas mass against the distance from the centre of each galaxy (see text for details).

an error in the dust temperature becomes very large even at the longest possible Herschel wavelength. Therefore, for this method to be practical at the highest redshifts, continuum measurements from the ground will be crucial.

Finally, we examine the potential of this method for estimating the distribution of the ISM within an individual galaxy, since the Atacama Large Millimetre Array will make it relatively easy to map the dust emission in a high-redshift galaxy. Figure 8 shows the ratio of the two estimates of the gas mass for each pixel plotted against distance from the centre of each galaxy. In making these estimates, we have used our best estimates of X and η_c (see above) and we have corrected for the inclination of each galaxy using the inclinations and position angles given in Chung et al. [2009]). There are clear radial gradients that were effectively averaged over when we carried out our global calibration. These gradients may be due to metallicity gradients, which can effect both methods (Magrini et al. 2011), or might be due to other effects such as the X factor for an individual galaxy being different from the standard value. In order to use either method as a reliable way of mapping the ISM in a high-redshift galaxy it will be crucial to understand the cause of these gradients. This will be very tricky because both the gas-to-dust factor and the X factor are likely to depend on metallicity (Wilson 1995; Lisenfeld and Ferrara 1998; James et al. 2002; Boselli et al. 2002; Israel 2005; Magrini et al. 2011). We believe progress is most likely to be made by measuring metallicity gradients for large numbers of galaxies with Herschel, HI and CO observations. Fortunately, despite the uncertainty in the absolute values of the metallicities of galaxies, most methods give similar results for the metallicity gradients (Moustakas et al. 2010; Magrini et al. 2011). Although the cause of these gradients is uncertain, the plots show again that the method of using the dust emission to map the ISM is a promising one. The r.m.s. dispersion of the log of the ratio of the two gas estimates around the best-fit lines in Figure 8 is 0.118, showing that, after a

correction is made for the gradients, the upper limit on the accuracy of one method (on the assumption that the other method is correct) is 31%, which is virtually the same as the accuracy for the global estimates. Since both methods rely on using tracers of the underlying gas (CO molecules and dust grain) and since there are observational errors in both cases, we believe the agreement between the two methods is remarkably good. Therefore, if the obstacle of understanding the cause of the gradients can be overcome, both methods should give consistent maps of the ISM in high-redshift galaxies.

Herschel is an ESA space observatory with science instruments provided by European-led Principal Investigator consortia with important participation from NASA. SPIRE has been developed by a consortium of institutes led by Cardiff Univ. (UK) and including Univ. Lethbridge (Canada); NAOC (China); CEA, LAM (France); IFSI, Univ. Padua (Italy); IAC (Spain); Stockholm Observatory (Sweden); Imperial College London, RAL, UCL-MSSL, UKATC, Univ. Sussex (UK); Caltech, JPL, NHSC, Univ. Colorado (USA). This development has been supported by national funding agencies: CSA (Canada); NAOC (China); CEA, CNES, CNRS (France); ASI (Italy); MCINN (Spain); Stockholm Observatory (Sweden); STFC (UK); and NASA (USA).

APPENDIX

THE RELATION BETWEEN SUBMILLIMETRE LUMINOSITY AND GAS MASS

The relationship obtained by the Planck team (Planck Collaboration 2011b) between the optical depth of submillimetre emission at a frequency ν and the column-density of hydrogen (measured in atoms cm^{-2}) is given by

$$\tau_\nu = 1.1 \times 10^{-25} \left(\frac{\lambda}{250 \mu\text{m}} \right)^{-1.8} N_H \quad (\text{A1})$$

We can translate this to a relationship between the submillimetre luminosity and the mass of gas using Kirchoff's Law:

$$j_\nu = \kappa_\nu B_\nu(T) \quad (\text{A2})$$

in which j_ν is the emissivity, κ_ν is the absorption coefficient and $B_\nu(T)$ is the Planck function. We assume that the dust is at a single constant temperature and that the dust is optically thin. The monochromatic submillimetre luminosity is then given by

$$L_\nu = \int j_\nu dV = B_\nu(T) \int \kappa_\nu dV \quad (\text{A3})$$

If x is the distance along the line-of-sight, the absorption coefficient is given by

$$\kappa_\nu = \frac{d\tau_\nu}{dx} = 1.1 \times 10^{-25} \left(\frac{\lambda}{250 \mu\text{m}} \right)^{-1.8} n_H \quad (\text{A4})$$

in which n_H is now the number of hydrogen atoms per cubic centimetre. By substituting A4 in A3, we obtain the relationship:

$$L_\nu = B_\nu(T) 1.1 \times 10^{-25} \left(\frac{\lambda}{250 \mu\text{m}} \right)^{-1.8} \int n_H dV \quad (\text{A5})$$

From which we obtain:

$$M_H = \frac{1.52 \times 10^2 \times L_\nu}{B_\nu(T_d) \times \left(\frac{\lambda}{250} \right)^{-1.8}} \quad (\text{A6})$$

in which we have converted everything into S.I. units except wavelength (λ), which is measured in microns. Luminosity is measured in Watts $\text{Hz}^{-1} \text{sr}^{-1}$. In this derivation we have assumed that the dust is precisely tracing the dust and has the same gas-to-dust ratio as in the Milky Way. If that is not the case, the constant of proportionality in equation A6 will simply scale with the gas-to-dust ratio.

REFERENCES

- Abdo, A. et al. 2010, ApJ, 710, 133
 Ackermann, M. et al. 2011, ApJ, 726, 81
 Ade, P. et al. 2011, arXiv:1101.2029
 Arimoto, N., Sofue, Y., Tsujimoto, T., 1996, PASJ, 48, 275
 Avni, Y. et al. 1976, ApJ, 210, 642
 Bell, T., Viti, S. & Williams, D. 2007, MNRAS, 378, 983
 Bendo, G.J. et al. 2010, MNRAS, 142, 1409
 Bendo, G. et al. 2011, in preparation
 Bolatto, A.D., Leroy, A.K., Rosolowsky, E., Walter, F. & Blitz, L. 2008, ApJ, 686, 948
 Boselli, A., Lequeux, J., Gavazzi, G., 2002, A&A, 384, 33
 Boselli, A. et al. 2010a, PASP, 122, 261
 Boselli, A., Ciesla, L., Buat, V., et al., 2010, A&A, 518, L61
 Braun, R., Thilker, D.A., Walterbos, R.A.M. & Corbelli, E. 2009, ApJ, 695, 937
 Boulanger, F., Abergel, A., Bernard, J.-P., Burton, W.B., Désert, F.-X., Hartmann, D., Lagache, G. & Puget, J.-L. 1996, A&A, 312, 256
 Chung, A., van Gorkom, J.H., Kenney, J.D.P., Crowl, H. & Vollmer, B. 2009, AJ, 138, 1741
 Davies, J. et al. 2010, *ã*, 518, L48
 Davies, J. et al. 2011, MNRAS, in press

- Draine, B.T. et al. 2003, *ARA&A*, 41, 241
Draine, B. et al. 2007, *ApJ*, 663, 866
Eales, S.A. et al. 2010a, *PASP*, 122, 499
Eales, S.A. et al. 2010b, *A&A*, 518, 62
Foyle, K. et al. 2011, *MNRAS*, in press
Fritz, J. et al. 2011, *A&A*, submitted
Galametz, M. et al. 2011, *A&A*, 532, 56
Griffin, M. et al. 2010, *A&A*, 518, L3
Guelin, M., Zylka, R., Mezger, P., Haslam, C., Kreysa, E., Lemke, R., Sievers, A., 1993, *A&A*, 279, L37
Guelin, M., Zylka, R., Mezger, P., Haslam, C., Kreysa, E., 1995, *A&A*, 298, L29
Hildebrand, R.H. 1983, *QJRAS*, 24, 267
Hughes, T. et al. in preparation
Israel, F. 1997, *A&A*, 328, 471
Israel, F., 2005, *A&A*, 438, 855
James, A., Dunne, L., Eales, S. & Edmunds, M. 2002, *MNRAS*, 335, 753
Kewley, L. & Ellison, S. 2008, *ApJ*, 681, 1183
Kuno, N. et al. 2007, *PASJ*, 59, 117
Lisenfeld & Ferrara 1998, *ApJ*, 496, 145
Magrini, L. et al. 2011, *A&A*, 535, 13
Moustakas, J., Kennicutt, R., Tremonti, C.A., Dale, D.A., Smith, J.T. & Calzetti, D. 2010, *ApJ*, 190, 233
Oliver, S. et al. in preparation
Pettini, M. & Pagel, B. 2004, *MNRAS*, 348, 59
Pilbratt, G.L. et al. 2010, *A&A*, 518, L1
Planck Collaboration 2011a: Planck Early Results. XIX. All-sky temperature and dust optical depth from Planck and IRAS. Constraints on the “dark gas” in our Galaxy. *A&A*, 536, 19
Planck Collaboration 2011b: Planck Early Results: Properties of the interstellar medium in the Galactic plane, *A&A*, in press (arXiv:astro-ph/1101.2032v1)
Planck Collaboration 2011c: Planck Early Results: XXIV. Dust in the diffuse interstellar medium and the Galactic halo, *A&A*, in press (arXiv:astro-ph/1101.2036v2)
Poglitsch, A. et al. 2010, *A&A*, 518, L2
Shetty, R., Kauffmann, J., Schnee, S., Goodman, A.A. & Ercolano, B. 2009a, *ApJ*, 696, 2234
Shetty, R., Kauffmann, J., Schnee, S. & Goodman, A. 2009b, *ApJ*, 696, 676
Smith, M. et al. 2011a, in preparation
Smith, M. et al. 2011b, in preparation
Wilson, C. 1995, *ApJ*, 448, L97